

Effects of Device Coupling on Haptic Performance

Colin Gallacher¹, John Willes², and Jozsef Kövecses³

Abstract— This electronic document is a live template. The various components of your paper [title, text, heads, etc.] are already defined on the style sheet, as illustrated by the portions given in this document.

I. INTRODUCTION

At the moment, performance evaluation of force feedback haptic devices presents a huge hurdle towards the general acceptance of haptic technologies by the public. The wide range of device mechanism and uses poses a seriously challenging task of evaluating how a device will perform.

Currently we evaluate the performance of devices based on respective quantifiable performance metrics for haptic systems. These haptic systems are analysed based on the device properties in the unpowered, powered, and interactive state [[Samur12]]. Still, we lack valuable quantitative metrics that consumers could use to evaluate the quality of a device akin to the ??? for sound systems or ??? for televisions. Progress has been made to characterize the performance of specific devices based on their ability to perform in specified tasks that are fairly universal for haptic applications based on psychophysical evaluation test-beds. These widely accepted tasks can be partitioned into navigation, manipulation, and selection tasks.

Theoretically, a device's ability to perform well in these tasks should correspond to the overall usability of the device and thus, if quantified, could represent a means to discern a 'good' device from a 'bad' device. The usage of tried psychophysical evaluation techniques such as the fitts' tapping test[insert reference], peg in hole tests, etc., allow for the quantification of a device performance based on the users ability to perform a task of varying difficulty in a specified time.

These techniques have preliminarily been shown to be an effective means of evaluating two very different devices to perform a desired tasks. However, these evaluations are based on an ad hoc usage of the device workspace to perform the required tasks. In this study we seek to perform preliminary investigations into the dependency of device performance while performing the same task at different locations in the workspace.

We seek to evaluate the forces that a device may impart upon a user to decrease their ability to accomplish a simple

yet universally navigational task of moving from one area of a workspace to another along a straight line. These forces will here on out be referred to as parasitic forces. The understanding of the nature of these parasitic forces will be generalized but will be further elaborated upon for the 2D case of a planar-five-bar mechanism. Finally, simulation will be compared to experimental results for the case of the five-bar-mechanism to determine if, and then to quantify by how much, the device performance for a standard navigational task is influenced by the trajectory.

The motivation for this study is to formalize the notion of parasitic forces resulting from the manipulator dynamics that can decrease performance as well as providing a groundwork for future studies to explore the reduction of parasitic forces using redundant mechanisms. While this may actually muddy the water in terms of providing a clear-cut answer to the problem of quantifying a haptic device, it may allow for users of pre-built devices to better utilise their existing workspace to increase device performance for specific tasks.

II. THEORETICAL BACKGROUND

To better familiarize the reader with the nature of the experiment, here we will elaborate on the background theory required for the study.

A. Fitts' Law and the tapping test

Drawing from Shannon's seminal information theory work, *Mathematical Theory of Communication*[[Shannon48]], Fitts hypothesised that the time it took for a human to accomplish a task was linearly proportional to the difficulty of the task [[Fitts54]]. The relationship Fitts devised is analogous to Shannon's Theorem [[Shannon48]] and is referred to as Fitts' Law:

$$MT = \frac{ID}{IP} \quad (1)$$

Where, MT is the measured time, ID , is termed the *Index of Difficulty* and, IP , the Index of Performance. The index of difficulty is defined as,

$$ID = \log_2 \left(\frac{2A}{W} \right) \quad (2)$$

ID , is a way of non-dimensionalizing the difficulty of a movement task and corresponds to the ratio of the distance of an object, A , to the characteristic width of the object, W . Fitts required users tap a stylus between two targets of varying distance and size while measuring the time taken to perform the task. A linear regression was then performed on the data providing a line of best fit.

*This work was not supported by any organization

¹Albert Author is with Faculty of Electrical Engineering, Mathematics and Computer Science, University of Twente, 7500 AE Enschede, The Netherlands albert.author@papercept.net

²Bernard D. Researcher is with the Department of Electrical Engineering, Wright State University, Dayton, OH 45435, USA b.d.researcher@ieee.org

$$MT = a + bID \quad (3)$$

The intercept, a , and slope, b , are empirically determined constants. The slope of this line, b , corresponds to the reciprocal of the *Index of Performance*, IP , and is assumed constant for the specific tool or device the user is operating with. The use of the \log_2 in (2) allows for the ratio of distance to object width (corresponding to the associated difficulty of a task) to be expressed in units of *bits*. Rearranging equation (1) to solve for IP we see the *Index of Performance*, IP , can be expressed in units of $\frac{\text{bits}}{\text{sec}}$.

Ideally the intercept, a , is zero and deviations can be seen to indicate inaccuracies in the model, though may also be attributed to other additive effects that increase the measured time of a task but are not directly related to the task itself (i.e. button pressing to start and stop the measured time).

The Fitts' Law model of human response time as a function of task difficulty in 1D has held up well against scientific scrutiny and the results have been replicated and expanded upon for the 2D Steering Law [[insert references]] and even somewhat so for the 3D cases[[insert references]]. The validity of Fitts' Law as a tool for measuring the performance of haptic devices and virtual displays has also been demonstrated [[insert references]]. For a more detailed introduction to the intricacies of Fitts' Law, including an attempt at a derivation of the equation from physical principals, the authors direct the reader to references [[insert citations]].

The form of Fitts' Law we will be using is referred to as Shannon's variation as it is suggested by a direct analogy with Shannon's information theorem and is expressed as:

$$MT = a + b \log_2 \left(\frac{A + W_e}{W_e} \right) \quad (4)$$

Where, W_e , is defined as the *Effective Target Width* [[Welford68]].

B. Dynamic Formulations and Representations

In order to gain insight into the role parasitic forces may have on a haptic user, we must first develop a dynamic representation of the device. This section aims to develop a generalized minimum representation for a haptic device that partitions the forces the device imparts on the user during navigation into those that exist within the *operational space* and those in an orthogonal space defined as the *admissible-motion space*. This representation is described in detail by Kovcses [[Kovcses08]].

The variational form of the system dynamics is expressed with the scalar equation:

$$\delta \hat{q}_a^T (M \dot{q}_a + c - \tau) = 0 \quad (5)$$

Here the inertia tensor, M , centrifugal and Coriolis forces, c , and the generalized torques, τ , are represented in the joint space. The vector form of the joint space dynamics is:

$$M \dot{q}_a + c = \tau \quad (6)$$

The joint space velocities are mapped to the *operational* and *admissible-motion* spaces via the transformation,

$$\dot{u} = R q_a \quad (7)$$

where $\dot{u} = [\dot{u}_{op} \dot{u}_{adm}]$ and $R = \begin{bmatrix} J \\ B \end{bmatrix}$. J is the *Jacobian* mapping the joint variables to the operational space coordinates. The operation space coordinates are associated with a space of constrained motion for the device end-effector. We impose that R must be invertible through the selection of the matrix B which maps the joint velocities to the admissible-motion space. This allows us to express the joint velocities as:

$$q_a = R^{-1} \dot{u} \quad (8)$$

The variations can then be expressed as:

$$\delta q_a = \delta u^T R^{-T} \quad (9)$$

The substitution of the above equation into [[insert number equation]] allows us to write the variational form of the system dynamics in terms of the operational and admissible-motion spaces.

$$\delta u^T R^{-T} (M \dot{q}_a + c - \tau) = 0 \quad (10)$$

The vector form of the operational and admissible-motion space dynamics is then written as:

$$R^{-T} M \dot{q}_a + R^{-T} c = R^{-T} \tau \quad (11)$$

Differentiation of equation [[insert equation number]] leads to the acceleration level relationship:

$$\dot{q}_a = R^{-1} \ddot{u} + R^{\dot{-1}} \dot{u} \quad (12)$$

Substitution of the above equation into equation [[insert equation number]] leads to the device dynamics represented in the operational and admissible-motion space with the kinematic parametrizations also represented in the operations/admissible-motion space realization.

$$R^{-T} M (R^{-1} \ddot{u} + R^{\dot{-1}} \dot{u}) + R^{-T} c = R^{-T} \tau \quad (13)$$

Expanding the above equation permits the device dynamics to be expressed as:

$$R^{-T} M R^{-1} \ddot{u} + R^{-T} M R^{\dot{-1}} \dot{u} + R^{-T} c = R^{-T} \tau \quad (14)$$

Grouping the acceleration and velocity terms together we arrive at the equation:

$$R^{-T} M R^{-1} \ddot{u} + R^{-T} \bar{c} = R^{-T} \tau \quad (15)$$

The first term corresponds to the inertial forces felt in the operational and admissible motion spaces as a result of the device acceleration.

$$f_1 = R^{-T} M R^{-1} \ddot{u} \quad (16)$$

The second term corresponds to the inertial forces associated with the device velocities often called the centrifugal and Coriolis forces.

$$\mathbf{f}_2 = \mathbf{R}^{-T} \bar{\mathbf{c}} \quad (17)$$

The term on the right hand side of equation [[insert equation number]] corresponds to the applied forces at the haptic end-effector with respect to the operational and admissible-motion spaces.

If we define $\mathbf{W} = \mathbf{R}^{-T} \mathbf{M} \mathbf{R}^{-1}$, $\mathbf{z} = \mathbf{R}^{-T} \bar{\mathbf{c}}$, and $\mathbf{s} = \mathbf{R}^{-T} \boldsymbol{\tau}$ we can rewrite the dynamic equations as:

$$\mathbf{W} \ddot{\mathbf{u}} + \mathbf{z} = \mathbf{s} \quad (18)$$

This can be represented in block matrix form as:

$$\begin{bmatrix} \mathbf{W}_{op} & \mathbf{W}_{oa} \\ \mathbf{W}_{ao} & \mathbf{W}_a \end{bmatrix} \begin{bmatrix} \ddot{\mathbf{u}}_{op} \\ \ddot{\mathbf{u}}_a \end{bmatrix} + \begin{bmatrix} \mathbf{z}_{op} \\ \mathbf{z}_a \end{bmatrix} = \begin{bmatrix} \mathbf{s}_{op} \\ \mathbf{s}_a \end{bmatrix} \quad (19)$$

Finally, the force that we feel in the admissible-motion space is the parasitic force that a user trying to navigate strictly in the operational space would feel for a haptic device. The dynamic equation associated with the parasitic forces is then written as:

$$\mathbf{W}_{ao} \ddot{\mathbf{u}}_{op} + \mathbf{W}_a \ddot{\mathbf{u}}_a + \mathbf{z}_a = \mathbf{s}_a \quad (20)$$

$$\ddot{\mathbf{u}}_a = \mathbf{W}_a^{-1} (\mathbf{s}_a - \mathbf{z}_a - \mathbf{W}_{ao} \ddot{\mathbf{u}}_{op}) \quad (21)$$

III. METHODS AND ASSUMPTIONS

In this study we seek to determine if a user of a haptic device travelling between two points is influenced by the coupling of the device inertia and to quantify changes in their ability to perform the task. We assume the user seeks to travel along a straight line between the starting and end point, ultimately coming to rest in the quickest time possible. This is a discrete form of a traditional tapping test and can be modelled suitable by Fitts' law [[insert reference here]].

By changing the navigational task to coincide with directions of varying coupling and comparing the *Index of Performance* of the user we can develop an understanding of the role of coupling on haptic performance. We aim to simulate the navigational task to theoretically predict the performance trends that may occur as well as what the largest contributing factors are to the parasitic forces experienced.

A. Simulation

To simulate the navigational task, the device dynamics for a parallel five-bar mechanism were developed and represented in a Cartesian coordinate frame attached to the base of the device. The dynamic parameters were produced in accordance with the specifications of the Quansar 2DOF planar pantograph. As we are interested in gaining insight about the effects of coupling on the device performance we use the quadratic form of the kinetic energy equation at unit magnitude to express the device inertia along the principle axes with respect to the base frame.

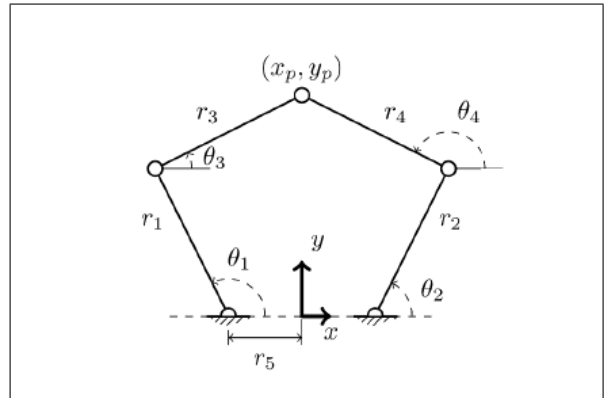


Fig. 1. Inductance of oscillation winding on amorphous magnetic core versus DC bias magnetic field

$$\mathbf{z}^T \mathbf{M} \mathbf{z} = \mathbf{z}^T \mathbf{P}^T \mathbf{D} \mathbf{P} \mathbf{z} = 1 \quad (22)$$

The column entries of \mathbf{P} represent the directions in the base frame along which the device inertia is decoupled. These directions are significant as an acceleration in a direction that is decoupled will not result in a parasitic force or subsequent acceleration in any orthogonal space. If there is a direction of minimum coupling, so too must there be a direction along which the coupling terms are maximum due to the invariance of the inertia dyad. These are of particular interest in determining the effects of coupling on device performance.

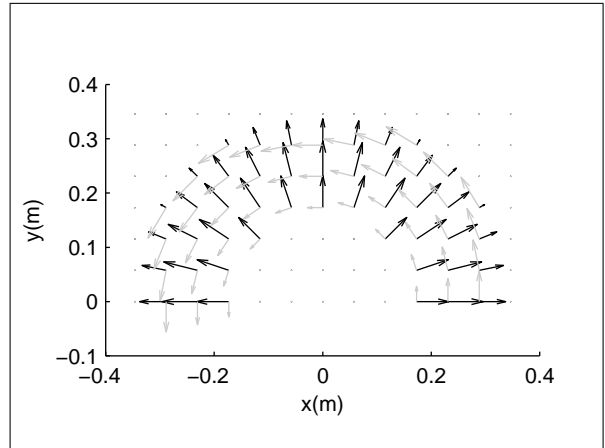


Fig. 2. Inductance of oscillation winding on amorphous magnetic core versus DC bias magnetic field

By performing a similarity transformation on the device inertia tensor, the directions along which maximum coupling occurs can be determined. This is analogous to computing the magnitude and directions of the maximum shear stress in solid mechanics[].

The directions and magnitude of the maximum coupling were computationally determined at each point in the device workspace. A contour map was procedurally generated with logarithms of the coupling magnitude and superimposed on a vector map of the directions of maximum coupling. This

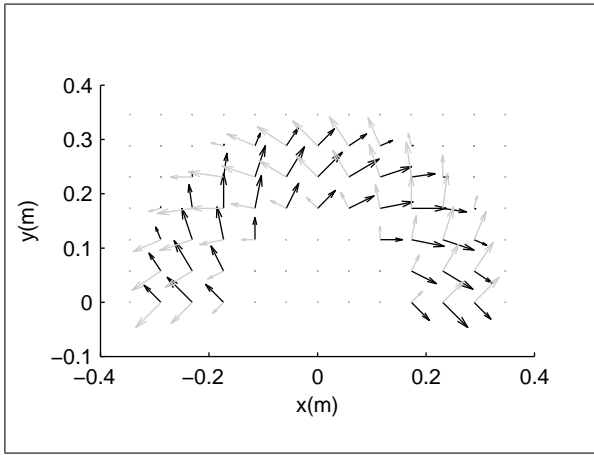


Fig. 3. Inductance of oscillation winding on amorphous magnetic core versus DC bias magnetic field

tool allowed us to select a region to simulate the navigation task as we wanted to minimize the effect that changes in the magnitude of the coupling had on path traversal. We felt this was important because operation within a region of too little coupling magnitude would have an insignificant impact on a user's performance regardless of path orientation. Simultaneously, we wanted to reduce changes in coupling magnitude while navigating to better isolate path orientation as the independent variable. While this is not perfectly realizable the selected paths can be seen below. The magnitude of the coupling is on the order of 10^{-2} - 10^{-4} kgs throughout the entire region of the path selection. This allows us to select a reasonably long path for the navigation task while in a roughly representative coupling magnitude range for the workspace. Three path orientations were selected based on the directions of coupling: (i) in the direction of inertia decoupling, (ii) in a direction corresponding to a high degree of inertia coupling, and (iii) a third direction that represents an arbitrary path neither along a decoupled or max coupled direction.

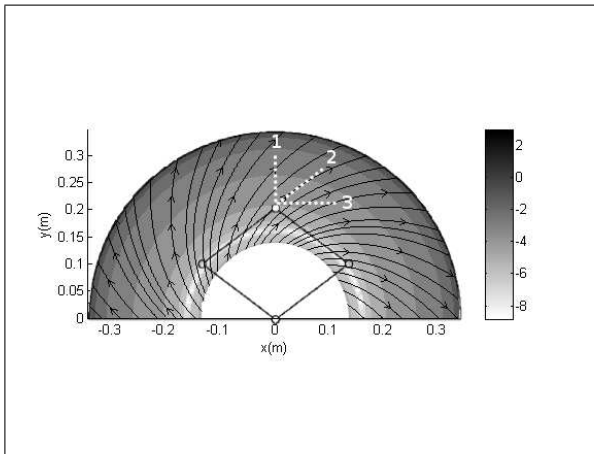


Fig. 4. Inductance of oscillation winding on amorphous magnetic core versus DC bias magnetic field

Next, the device dynamics are transformed into a min-

imum representation as described in Section 2b. We define the *operational space* as the direction along the line between the two points as this is the user's intended path of minimum length. The direction orthogonal to the *operational space* is the *admissible motion space*.

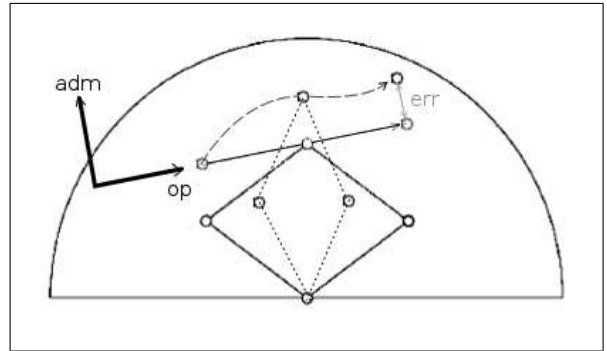


Fig. 5. Inductance of oscillation winding on amorphous magnetic core versus DC bias magnetic field

Our primary assumption in simulation is that the user does not provide feedback to correct for deviations from the path that may result from the device dynamics. This assumption is based on the evidence that a user performing rapid navigational tasks with a low *Index of Difficulty* do so ballistically (i.e. without feedback control) [[insert citation]]. Thus we prescribe a constant acceleration in the *operational space* but do not constrain movement in the admissible motion space.

Due to the restriction that the user must come to rest at the end of their journey, the acceleration in the operational space is reversed after half the operational path length, or rather, when the projection of the simulated trajectory onto the operational space is greater than half the distance of the line between the two points.

The accelerations were determined by performing a tapping test with an untethered stylus. The average duration it took for participants to tap between 10cm targets were between 0.36 and 0.44 seconds. We use this information and the path length to solve for a reasonable range for human acceleration.

We perform the simulations moving along the path for each orientation angle, $(\frac{pi}{2}, \frac{pi}{4}, 0)$ rads, while varying the operational space accelerations, $(0.27, 0.25, 0.23) \frac{m}{s^2}$, for each test. The simulations were then carried out for the reverse direction.

Finally, to examine the effects of the inertial forces resulting from acceleration opposed to those resulting from velocity, the simulations were carried out again with a constant velocity for the same duration of time (the average velocities from the original tests).

B. Experiments

Human experiments were performed to validate the simulations using the Quansar 2DOF planar pantograph. The testbed was setup using the same path lengths and orientations as those simulated. Users were asked to traverse

the path as quickly and accurately as possible. They then performed the navigational tasks in the reverse direction. Small, 1cm, and large, 2cm, diameter targets were chosen in accordance with Fitts' law to provide variation in the time it took for users to complete the navigation task, thus emulating variation in acceleration.

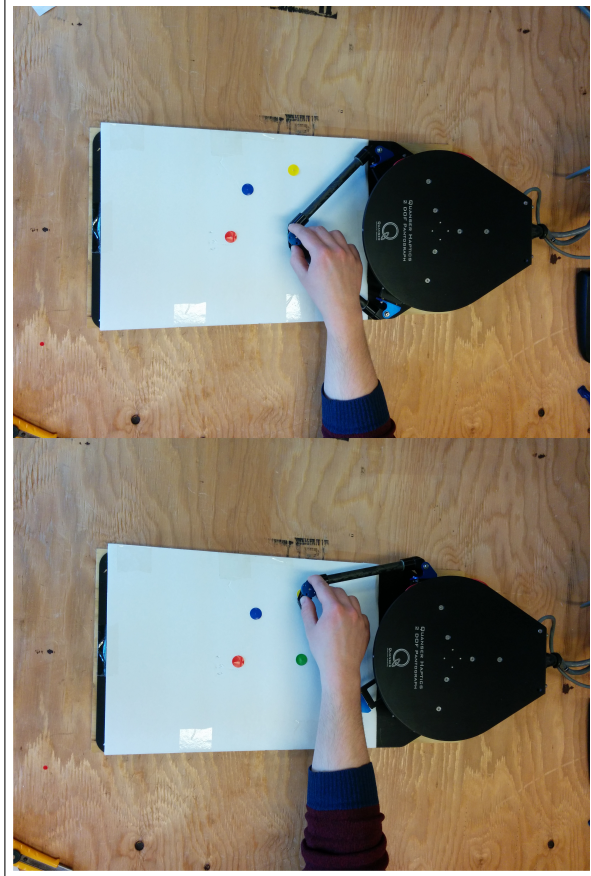


Fig. 6. Inductance of oscillation winding on amorphous magnetic core versus DC bias magnetic field

IV. RESULTS

Use this sample document as your *LaTeX* source file to create your document. Save this file as **root.tex**. You have to make sure to use the *cls* file that came with this distribution. If you use a different style file, you cannot expect to get required margins. Note also that when you are creating your out PDF file, the source file is only part of the equation. *Your TeX → PDF filter determines the output file size. Even if you make all the specifications to output a letter file in the source - if your filter is set to produce A4, you will only get A4 output.*

It is impossible to account for all possible situation, one would encounter using *TeX*. If you are using multiple *TeX* files you must make sure that the “MAIN” source file is called *root.tex* - this is particularly important if your conference is using PaperPlaza’s built in *TeX* to PDF conversion tool.

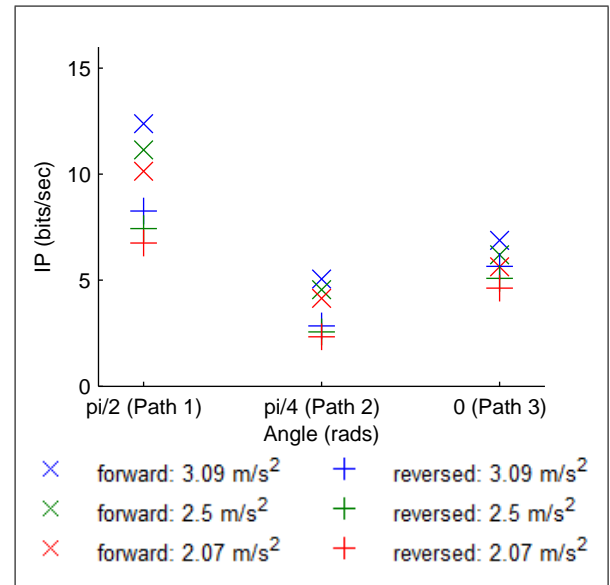


Fig. 7. Inductance of oscillation winding on amorphous magnetic core versus DC bias magnetic field

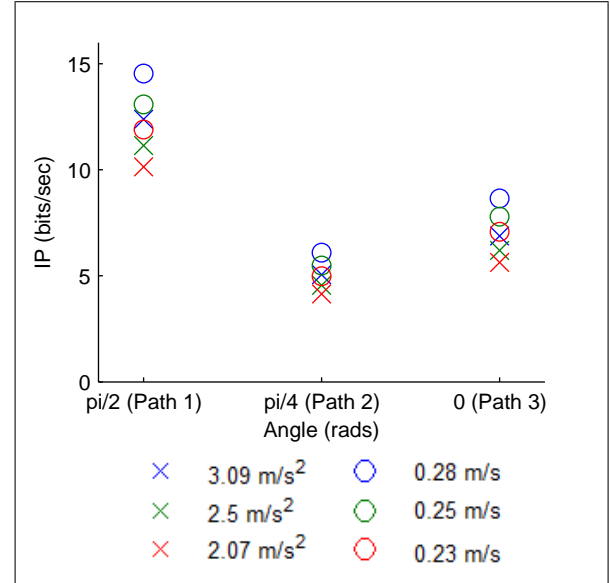


Fig. 8. Inductance of oscillation winding on amorphous magnetic core versus DC bias magnetic field

A. Headings, etc

Text heads organize the topics on a relational, hierarchical basis. For example, the paper title is the primary text head because all subsequent material relates and elaborates on this one topic. If there are two or more sub-topics, the next level head (uppercase Roman numerals) should be used and, conversely, if there are not at least two sub-topics, then no subheads should be introduced. Styles named Heading 1, Heading 2, Heading 3, and Heading 4 are prescribed.

B. Figures and Tables

Positioning Figures and Tables: Place figures and tables at the top and bottom of columns. Avoid placing them in the middle of columns. Large figures and tables may span across

both columns. Figure captions should be below the figures; table heads should appear above the tables. Insert figures and tables after they are cited in the text. Use the abbreviation Fig. 1, even at the beginning of a sentence.

TABLE I
AN EXAMPLE OF A TABLE

One	Two
Three	Four

We suggest that you use a text box to insert a graphic (which is ideally a 300 dpi TIFF or EPS file, with all fonts embedded) because, in an document, this method is somewhat more stable than directly inserting a picture.

Fig. 9. Inductance of oscillation winding on amorphous magnetic core versus DC bias magnetic field

Figure Labels: Use 8 point Times New Roman for Figure labels. Use words rather than symbols or abbreviations when writing Figure axis labels to avoid confusing the reader. As an example, write the quantity Magnetization, or Magnetization, M, not just M. If including units in the label, present them within parentheses. Do not label axes only with units. In the example, write Magnetization (A/m) or Magnetization A[m(1)], not just A/m. Do not label axes with a ratio of quantities and units. For example, write Temperature (K), not Temperature/K.

V. CONCLUSIONS

A conclusion section is not required. Although a conclusion may review the main points of the paper, do not replicate the abstract as the conclusion. A conclusion might elaborate on the importance of the work or suggest applications and extensions.

APPENDIX

Appendices should appear before the acknowledgment.

ACKNOWLEDGMENT

The preferred spelling of the word acknowledgment in America is without an e after the g. Avoid the stilted expression, One of us (R. B. G.) thanks . . . Instead, try R. B. G. thanks. Put sponsor acknowledgments in the unnumbered footnote on the first page.

References are important to the reader; therefore, each citation must be complete and correct. If at all possible, references should be commonly available publications.

REFERENCES

- [1] G. O. Young, Synthetic structure of industrial plastics (Book style with paper title and editor), in Plastics, 2nd ed. vol. 3, J. Peters, Ed. New York: McGraw-Hill, 1964, pp. 1564.
- [2] W.-K. Chen, Linear Networks and Systems (Book style). Belmont, CA: Wadsworth, 1993, pp. 123135.
- [3] H. Poor, An Introduction to Signal Detection and Estimation. New York: Springer-Verlag, 1985, ch. 4.
- [4] B. Smith, An approach to graphs of linear forms (Unpublished work style), unpublished.
- [5] E. H. Miller, A note on reflector arrays (Periodical styleAccepted for publication), IEEE Trans. Antennas Propagat., to be published.
- [6] J. Wang, Fundamentals of erbium-doped fiber amplifiers arrays (Periodical styleSubmitted for publication), IEEE J. Quantum Electron., submitted for publication.
- [7] C. J. Kaufman, Rocky Mountain Research Lab., Boulder, CO, private communication, May 1995.
- [8] Y. Yorozu, M. Hirano, K. Oka, and Y. Tagawa, Electron spectroscopy studies on magneto-optical media and plastic substrate interfaces (Translation Journals style), IEEE Transl. J. Magn.Jpn., vol. 2, Aug. 1987, pp. 740741 [Dig. 9th Annu. Conf. Magnetics Japan, 1982, p. 301].
- [9] M. Young, The Technical Writers Handbook. Mill Valley, CA: University Science, 1989.
- [10] J. U. Duncombe, Infrared navigationPart I: An assessment of feasibility (Periodical style), IEEE Trans. Electron Devices, vol. ED-11, pp. 3439, Jan. 1959.
- [11] S. Chen, B. Mulgrew, and P. M. Grant, A clustering technique for digital communications channel equalization using radial basis function networks, IEEE Trans. Neural Networks, vol. 4, pp. 570578, July 1993.
- [12] R. W. Lucky, Automatic equalization for digital communication, Bell Syst. Tech. J., vol. 44, no. 4, pp. 547588, Apr. 1965.
- [13] S. P. Bingulac, On the compatibility of adaptive controllers (Published Conference Proceedings style), in Proc. 4th Annu. Allerton Conf. Circuits and Systems Theory, New York, 1994, pp. 816.
- [14] G. R. Faulhaber, Design of service systems with priority reservation, in Conf. Rec. 1995 IEEE Int. Conf. Communications, pp. 38.
- [15] W. D. Doyle, Magnetization reversal in films with biaxial anisotropy, in 1987 Proc. INTERMAG Conf., pp. 2.2-12.2-6.
- [16] G. W. Juette and L. E. Zeffanella, Radio noise currents n short sections on bundle conductors (Presented Conference Paper style), presented at the IEEE Summer power Meeting, Dallas, TX, June 2227, 1990, Paper 90 SM 690-0 PWRS.
- [17] J. G. Kreifeldt, An analysis of surface-detected EMG as an amplitude-modulated noise, presented at the 1989 Int. Conf. Medicine and Biological Engineering, Chicago, IL.
- [18] J. Williams, Narrow-band analyzer (Thesis or Dissertation style), Ph.D. dissertation, Dept. Elect. Eng., Harvard Univ., Cambridge, MA, 1993.
- [19] N. Kawasaki, Parametric study of thermal and chemical nonequilibrium nozzle flow, M.S. thesis, Dept. Electron. Eng., Osaka Univ., Osaka, Japan, 1993.
- [20] J. P. Wilkinson, Nonlinear resonant circuit devices (Patent style), U.S. Patent 3 624 12, July 16, 1990.